

# Optimizing ssNMR experiments for dilute proteins in heterogeneous mixtures at high magnetic fields

Seth A. McNeill,<sup>1</sup> Peter L. Gor'kov,<sup>2</sup> Jochem Struppe,<sup>3</sup> William W. Brey<sup>2</sup> and Joanna R. Long<sup>1\*</sup>

<sup>1</sup> Department of Biochemistry and Molecular Biology, McKnight Brain Institute, Department of Electrical and Computer Engineering, University of Florida, Gainesville, FL 32610, USA

<sup>2</sup> National High Magnetic Field Laboratory, Tallahassee, FL 32310, USA

<sup>3</sup> Bruker Biospin Corp., Billerica, MA, USA

Received 22 June 2007; Revised 1 October 2007; Accepted 16 October 2007

**Solid-state NMR spectroscopy at high magnetic fields is proving to be an effective technique in structural biology, particularly for proteins which are not amenable to traditional X-ray and solution NMR approaches. Several parameters can be selected to provide optimal sensitivity, improve sample stability, and ensure biological relevance for ssNMR measurements on protein samples. These include selection of sample conditions, NMR probe design, and design of pulse experiments. Here, we demonstrate and evaluate several engineering and experimental approaches for pursuing measurements on dilute proteins in heterogeneous mixtures. Copyright © 2007 John Wiley & Sons, Ltd.**

**KEYWORDS:** solid-state NMR; membrane proteins; probe design; pulse sequence; sample heating; low-E

## INTRODUCTION

High-resolution NMR has proven invaluable in the determination of structure and dynamics for small molecules as well as large biomolecular complexes, including proteins. However, its success hinges on being able to identify solvent conditions for which the molecule studied tumbles isotropically on the NMR timescale in order to average chemical shifts to their isotropic values and to minimize the effects of dipolar and quadrupolar couplings on spectroscopic resolution. The averaging of these interactions by molecular tumbling makes the design of NMR experiments and their interpretation reasonably straightforward. Thus, most commercial instruments are now supplied with the hardware and software capabilities necessary for full structure determination of soluble proteins once a few basic parameters, such as r.f. pulse calibrations, have been measured and input into the routines. Unfortunately, many systems of interest to chemists and structural biologists are not amenable to this approach.

Solid-state NMR (ssNMR) spectroscopy is unique in its ability to measure *in situ* the structure and dynamics of insoluble complexes at atomic level resolution. The major drawback and advantage of ssNMR is that the spatial components of the NMR interactions are no longer averaged to zero. These interactions contain valuable information about the structure, dynamics, and organization of molecules in a sample, but they also lead to broad featureless spectra. In order to render the problem of resolution tractable, it is

necessary to remove or reduce the anisotropic interactions by orienting the molecules, applying a strong and precisely controlled r.f. magnetic field, mechanically rotating the sample about an angle (the so-called magic angle), or by a combination of these techniques. However, all the interactions of interest can then be brought back through careful and creative choices of sample conditions and pulse experiments to achieve detailed measurements of the structure and dynamics of the molecules in a sample at atomic resolution.

Given the complexities involved, ssNMR is often viewed by the larger scientific and medical communities as technically challenging and requiring excessive effort to successfully address problems of chemical and biological interest. However, with the advent of molecular biological techniques for generating larger, isotopically enriched quantities of previously difficult, insoluble proteins and the standardization and maturation of commercial digital NMR instruments, this perception is no longer as true as it was in the 1980s and even 1990s. These developments, coupled with increases in magnetic fields, improvement in pulse techniques, and a better understanding of the underlying physics, place ssNMR in the position of being able to address several important and previously intractable problems in chemical biology.

The ability to study protein structure and dynamics in heterogeneous systems at atomic resolution provides exciting opportunities for determining the relationship between structure and function in native matrices, such as lipid bilayers<sup>1–3</sup> and spider silk,<sup>4,5</sup> as well as in designed environments.<sup>6</sup> The structure and dynamics of protein immobilization is a central theme in fields ranging from structural biology to nanotechnology to medical diagnostics.

\*Correspondence to: Joanna R. Long, Department of Biochemistry and Molecular Biology, McKnight Brain Institute, University of Florida, Gainesville, FL 32610, USA. E-mail: jrlong@mbi.ufl.edu

ssNMR can examine the structure and dynamics of these proteins at an atomic level under a wide variety of solvation states, providing new insights into their function.

### APPROACHES TO SOLVING GLOBAL PROTEIN STRUCTURE BY SSNMR

In recent years, much of the focus in the biomolecular ssNMR community has been on developing magic angle spinning (MAS) methodologies for global determination of protein structure.<sup>7–14</sup> These studies have primarily utilized multidimensional NMR experiments to determine through-space and through-bond interactions, much like high-resolution NMR studies of soluble proteins. Spin–spin correlations provide relative information on connectivity and distances between atoms in a protein, which is useful in assigning resonances and providing structural constraints. Chemical shift measurements allow qualitative calculations of local secondary structures as additional constraints. By measuring the isotropic and anisotropic chemical shifts as well as spin–spin correlations via *J*- and dipolar couplings, several globular proteins have been fully assigned and their structures determined to high resolution. The success of this approach relies on obtaining hundreds or thousands of constraints for even small proteins. When a protein exists in an array of structures or in an extended type structure, these measurements are not able to determine structure as accurately. Coherence measurements can then be used to obtain quantitative distances between specific atoms in order to refine an extended structure or to determine conformational heterogeneity.

These studies have been particularly successful for nanocrystalline samples. Nanocrystalline protein samples can lack the long-range order necessary for X-ray diffraction studies yet have the necessary uniformity and resolution for MAS ssNMR measurements.<sup>10,12,15</sup> Often these nanocrystals can be created using precipitation techniques that require less than an hour as compared to the days or weeks necessary for diffraction quality crystals. Samples created by fibrillarization, freezing, or lyophilization have also been studied,<sup>16–18</sup> but quite often their resolution is compromised owing to line broadening from side-chain conformational variability as well as other inhomogeneous broadening mechanisms. In many cases, <sup>13</sup>C linewidths in fully labeled proteins are greater than 0.25 ppm, resulting in unresolvable resonances that are inextricable for assignment. Some of these challenges can be overcome through the use of selective labeling schemes and higher experiment dimensions, at the expense of increasing the number of samples and experiments. However, the linewidths of these samples also provide important information on the degree of short-range order in amorphous samples.

Proteins that are pure and aggregated or in microcrystalline form are typically analyzed via single-quantum experiments or double-quantum experiments with coherences excited between directly bonded spins. By the nature of their physical state they are available as small, highly concentrated samples. To study these samples, it is best to use small sample containers (rotors) and detection coils to

obtain high sensitivity per unit mass.<sup>19</sup> These small dimensions also provide other advantages such as large r.f. fields and high sample rotation rates. However, for many systems this approach does not provide a biologically relevant environment for the protein.

One approach in applying ssNMR to the study of membrane proteins is to use mechanically or magnetically aligned samples.<sup>2,20–22</sup> Structural restraints are derived from observations of a range of anisotropic nuclear spin interactions (e.g. chemical shifts and nuclear spin dipolar interactions) from aligned samples that have a unique orientation with respect to the applied magnetic fields. In these experiments, multiple thin glass plates or liquid crystalline media (such as bicelles) are used to macroscopically align protein or peptide-containing lipid bilayers. The sealed, sample cells needed to maintain the correct hydration levels take up further space within the r.f. coil. The combination of low protein concentrations and low filling factor often mandates use of large coil volumes (200 to 500 mm<sup>3</sup>) to produce sufficient signal-to-noise ratio (S/N). Polarization inversion spin exchange at the magic angle (PISEMA) and related sequences can then be used to obtain orientational restraints and these restraints can be combined to determine a membrane protein structure.<sup>23–25</sup>

### SPECIAL CONSIDERATIONS FOR PROTEINS IN HETEROGENEOUS ENVIRONMENTS

Often, when studying protein structure and dynamics, the question is how a protein functions in a particular environment or alters its environment. For example, membrane-associated proteins make up approximately 30% of the human genome and play key roles in signal transduction and membrane organization. Since standard X-ray crystallography and liquid NMR techniques only work for the water-soluble portions of the proteins or proteins solubilized in a detergent, sample preparation often leads to the proteins being inactivated (e.g. the X-ray structure of rhodopsin crystallized from detergent<sup>26</sup>) or constitutively activated (e.g. the crystal structure of only the extracellular domains of  $\alpha_v\beta_3$  integrin<sup>27</sup>). Therefore, determining the relationship between structure and function is hindered. Additionally, information on the complex dynamics of these proteins and the lipids with which they interact is lacking. Gaining insights into the structure and dynamics of membrane-associated proteins in their native lipid environment is necessary both for understanding the functional mechanisms of these proteins as well as the importance of membrane fluidity, individual lipids, fatty acids, and small molecules in protein function. Two areas of interest in membrane protein biology that can be uniquely addressed by ssNMR are the influence of membrane composition on protein function and the roles of specific proteins in influencing membrane properties.

Especially striking examples of the ability of proteins to regulate the physical properties of lipids are the pulmonary surfactant proteins. The alveoli are lined with a specialized extracellular film comprising lipids and proteins known as lung surfactant to lower their surface tension. It is now established that lung surfactant proteins, while comprising less than 10% by weight of lung surfactant, are essential for

the properties of the lung during cyclic compression and expansion.<sup>28</sup> In fact, the proteins behave in a concentration- and lipid-dependent manner when interacting with lipid membranes.<sup>29</sup> In order for the NMR measurements to be of biological relevance, the lipid : peptide ratio must exceed 30:1. Thus, for hydrated samples, a particular protein comprises <1% by mass of the sample and poses significant challenges for both sensitivity and dynamic range since even unenriched lipids contain significant amounts of natural-abundance <sup>13</sup>C spins. Additionally, these proteins can decrease alignment in lipid systems which would have spontaneously aligned in the absence of protein. The result is that these proteins are not amenable to study by NMR techniques that rely on macroscopic alignment of the sample with the magnetic field.

In larger organisms, the organization of extracellular matrix proteins is critical to the formation of connective tissue, skeletal growth, signaling, and nutrient transport. Extracellular matrix is characterized by hierarchical organization of proteins and lipids into insoluble networks which are not amenable to standard structural biology techniques. However, NMR is capable of studying the organization and function of these proteins at an atomic level as well as transport properties of small molecules in these complex networks. One example of this is the study of protein-mediated mineral formation and remodeling. Because of the complex, heterogeneous nature of biomineralization, little is understood about the biological regulation of the proteins involved or the molecular basis for their action in hydroxyapatite (HAP) formation and regulation. Using NMR, a systematic examination of the molecular structure and dynamics of mineralization peptides and proteins in their native environments and their influence on the diffusion properties of small molecules is possible and can elucidate the mechanisms underlying mineralization in bone.<sup>30–35</sup> In these studies the proteins are first adsorbed onto the mineral of interest and then packed in a sample rotor for study. For adsorbed proteins, a rule-of-thumb for estimating the amount of protein present in a sample is that at monolayer coverage about 1 mg of protein adsorbs per square meter of support. Although it is possible to generate substrates with surface areas greater than 100 m<sup>2</sup>/g, typically the protein-accessible surface areas are substantially lower.

Protein immobilization on polymeric surfaces is being explored for biomaterials development, tissue engineering, drug delivery, affinity separations, and the advancement of diagnostic tools. However, because most polymers with ideal mechanical properties are hydrophobic, soluble proteins tend to denature on adsorption to their surfaces. In order to design proteins with enhanced attachment properties that can maintain function upon adsorption, a better understanding of the fundamental mechanisms of protein adsorption is needed. Only ssNMR can examine the structure and dynamics of adsorbed proteins at an atomic level under a wide variety of solvation states.<sup>6,30</sup> In the biosensor arena, phage and cell surface display technologies have enabled the identification of peptide sequences with affinities for specific inorganic materials, most notably electronic materials, to be identified. However, studies examining the molecular

bases of these binding events and how the interactions might couple the peptides to electronics have been limited and primarily phenomenological rather than quantitative. Mechanisms of peptide binding to inorganic surfaces, design of optimal sequences for controllable adsorption (and desorption), and stability of the biopolymer–inorganic interfaces can be examined via ssNMR.<sup>36</sup>

These are just a few examples of heterogeneous samples in which the protein of interest is inherently dilute. In maximizing signal of dilute samples, the focus moves from sensitivity per unit mass to how sensitivity scales with volume. Since these samples are concentration limited rather than mass limited, larger sample volumes can lead to significant improvements in S/N. An additional consideration for these samples is improving the dynamic range and accuracy of coherent measurements in order to obtain high-resolution structural measurements. Selective isotopic enrichment allows significant improvements in single-quantum experiments, but accurate measurements still require careful subtraction of natural abundance contributions from the rest of the protein as well as the surrounding medium. Double-quantum filtered experiments can successfully remove natural abundance signals and significantly improve the accuracy of structural measurements.<sup>32</sup> A final consideration in examining heterogeneous samples is that quite often the spectra of proteins will have lower resolution than crystalline samples, either due to structural or environmental heterogeneity, and possibly dynamics, confounding pulse experiments. Nonetheless, coherence measurements can be successfully carried out to answer mechanistic questions and dynamics can be determined by either sideband analysis in slow-spinning experiments or relaxation measurements.

## BIOLOGICAL SSNMR AT HIGH MAGNETIC FIELDS

NMR is fundamentally an insensitive spectroscopy; however, with the ability to engineer increasingly larger, stable, homogenous fields, the applicability of ssNMR to biological systems has significantly increased. When sample loss is negligible, for spin 1/2 nuclei gain in sensitivity with increasing the magnetic field scales as  $B_0^{7/4}$ .<sup>19</sup> Although many ssNMR experiments have been successfully carried out at 500 MHz, there are significant limitations that are alleviated at higher field strength. Even for larger samples, the time required at 500 MHz to accumulate a sufficient number of signal averages, typically at least several days, can compromise the integrity of the samples. Study of samples with <100 nmoles of the spin of interest is simply unrealistic at 11.7 T. A conservative estimate of increasing S/N a factor of 1.8 or 2.8 in moving experiments from 500 to 700 or 900 MHz allows structural measurements, which take 7–10 days to complete at 500 MHz, to be accomplished in 1–3 days. Not only does this allow more efficient utilization of instrumentation and speed up scientific progress, but problems with sample integrity due to the inherent, time-dependent degradation of many hydrated biological samples can be abrogated.

Additional benefits of moving to higher fields are enhanced resolution and more accurate measurements of chemical shift anisotropies (CSAs) due to the linear scaling of chemical shift with  $B_0$ .<sup>37</sup> The increased frequency also allows better selectivity for resonance-specific excitation. However, this benefit also presents a challenge since spins resonant over a larger range of frequencies must be evenly manipulated, requiring stronger r.f.-generated  $B_1$  fields. A major challenge in ssNMR is dealing with the increasing anisotropic interactions as  $B_0$  increases (Fig. 1). While dipolar fields remain constant on moving to higher magnetic fields, isotropic and anisotropic chemical shift interactions scale linearly. Thus, a typical 200 ppm carbon chemical shift spectrum corresponds to 45 kHz at 21 T and a 150 ppm carbonyl carbon CSA corresponds to 34 kHz. For this reason, averaging of the CSAs via MAS requires faster spinning speeds at high fields.<sup>38</sup> While technological improvements in MAS have aided in averaging CSAs, sufficient r.f. must be delivered to the sample to fully excite all spins of interest. This problem is amplified for multipulse sequences designed with the intention of retaining small dipolar couplings between spins while averaging CSAs over long mixing times. Available r.f. power is one limitation on  $B_1$  that can be addressed with the purchase of r.f. power amplifiers. A more fundamental restriction on  $B_1$  is the tendency of r.f. components to arc with the large voltages present due to high power through reactive electrical elements. The potential for arcing is even more significant in standard bore magnets where less space is available for large, high voltage components.

Balancing the demands of high  $B_1$  fields (i.e. shorter pulses) and faster spinning speeds with choosing a probe optimized for sensitivity to either mass-limited or to concentration-limited samples is the focus of our analyses presented below. Of particular interest is minimizing the detrimental effects of sample heating due to strong r.f. fields and friction due to MAS. In order to gain the structural information desired for understanding protein structure and dynamics, selection of pulse sequence experiments in the context of high magnetic fields and samples of finite stability is also discussed.

## BIOLOGICAL SSNMR PROBE DESIGN CONSIDERATIONS

The purchase of a high-field NMR spectrometer and magnet system is one of the more expensive undertakings in structural biology. This is counteracted by sensitivity gains and the long-term stability of the magnet (often >20 years). However, for any NMR system, the r.f. probe is an equally important component. For biological ssNMR systems, probes must meet several criteria simultaneously: they must be able to produce sufficient and uniform nutation rates for  $^1\text{H}$  and other nuclei; they must provide adequate sensitivity, largely by having a large enough active volume within the sample coil; they must minimize sample heating during the delivery of r.f. pulses to a level that will not dehydrate or otherwise damage the samples; and MAS probes must also be capable of rotating the sample at a sufficient rate.

Typically, biological ssNMR experiments require NMR probes tuned to two or three frequencies –  $^1\text{H}$ ,  $^{13}\text{C}$  and/or  $^{15}\text{N}$ . The proton channel is particularly important since a high  $B_1$  field for proton decoupling is required to remove the detrimental broadening effects of proton dipolar couplings on the typically observed, lower-gamma  $^{13}\text{C}$  and  $^{15}\text{N}$  resonance linewidths.<sup>39,40</sup> Thus, probes are optimal if sensitivity is maximized for the lower frequency channels and the  $^1\text{H}$  channel can provide  $B_1$  fields of  $\sim 100$  kHz sustainable for decoupling and mixing periods of 20 ms or longer. The efficiency of the  $^1\text{H}$  channel is important insofar as a less efficient probe will require a higher power amplifier to produce the same  $B_1$ . However, if a sufficiently powerful  $^1\text{H}$  amplifier is available, it is advantageous to trade off  $^1\text{H}$  channel efficiency for  $^{13}\text{C}$  or  $^{15}\text{N}$  sensitivity.

Another key attribute of the probe is that the  $B_1$  field of the  $^1\text{H}$  channel be able to match that of the lower frequency channels to satisfy the Hartmann–Hahn condition<sup>41</sup> across the entire sample to allow maximum polarization transfer efficiency from the proton bath to the lower gamma nuclei during cross-polarization (CP). A simple way to ensure this is to use a single, multiply resonant sample coil.<sup>42</sup> However, during many multipulse sequences on the lower gamma channels, it is critical that the  $^1\text{H}$  decoupling be sufficiently high at all points in the sample that the Hartmann–Hahn condition is *not* met to prevent polarization transfer back to the proton bath from the lower gamma nuclei.<sup>40</sup> In order to achieve good sensitivity for the  $^{13}\text{C}$  or  $^{15}\text{N}$  channel, multiturn solenoids having a relatively high inductance are often used. The same solenoid may not be as efficient or well suited for the  $^1\text{H}$  frequency, which is as much as  $10\times$  higher. In particular, as the electrical length of the coil approaches  $1/4$  of the wavelength of the  $^1\text{H}$  frequency, standing waves in the solenoid can become significant and lead to severe  $B_1$  inhomogeneity in the proton channel.<sup>43–45</sup> Not only does this affect polarization transfer efficiency but it also leads to nonideal evolution of the magnetization during multipulse sequences and thus attenuates magnetization transfer and limits accuracy when measuring small internuclear couplings. It is possible to shift the standing wave so that the current maximum coincides with the center of the coil by modifying the circuit so that each end of the coil sees the same impedance with respect to ground. This measure, known as balancing the coil, greatly improves the  $B_1$  homogeneity, and it also reduces to half the voltage to ground on the driven side of the coil.

The use of high-inductance, multiturn coils for the  $^1\text{H}$  channel leads to other problems as well. The high voltage developed across the sample coil interacts with the dielectric constant of the sample, producing large frequency shifts of probe resonance upon sample insertion. Thus, frequent modifications of probe circuitry are required in order to accommodate a wide range of sample conditions. More importantly, r.f. loss in partially conductive sample reduces the achievable  $B_1$  field.<sup>46</sup> A larger r.f. power amplifier may be required to make up the difference. Larger sample volumes exacerbate this problem. In a 470  $\mu\text{l}$  solenoid at 600 MHz, for example, proton  $B_1$  fields at a given power level can vary by up to a factor of 2 depending on the sample in the coil.<sup>45</sup>

As a result, the optimum parameters keep changing from one sample to another, leading to a significant amount of extra spectrometer time and effort to keep a pulse sequence optimized for biological samples with low sensitivity.

However, the most important drawback of using multiturn solenoids for  $^1\text{H}$  irradiation is that the large electric field required to drive current through the solenoid will also heat the sample.<sup>47–49</sup> Biological systems are unique in that they are versatile and highly specialized under ambient conditions. The distinctive structure and dynamics in proteins are in large part due to nonbonded, intramolecular contacts, such as hydrogen-bonding and hydrophobic interactions. The stability of these contacts is thermally limited, and significant changes in temperature (10–50 K for room temperature samples) can overpower these weaker interactions, leading to proteins which are temporarily, or, quite often, permanently denatured. Some amount of sample heating inevitably accompanies the generation of high  $B_1$  fields needed for NMR. However, much more sample heating can arise from the use of high-inductance coils that require high voltages, and therefore, large electric fields, to produce sufficient  $B_1$ . In ssNMR, the principal drawback to r.f. loss is sample heating. In MRI and *in vivo* spectroscopy, the more important issue is the concomitant loss in efficiency and probe quality factor,<sup>50</sup> but the physical basis is the same. Balancing the coil, as described above, does not help reduce interaction of the sample with the coil's electric field since it does not reduce the voltage across the coil.

The electric field in the sample during an r.f. pulse can be thought of as having two independent components. There is an electric field component that is produced by the time fluctuations of the magnetic field that is needed to manipulate the atomic spins. This electric field curls around the lines of magnetic induction. The second component of the electric field is due to the voltage across the r.f. coil. When r.f. power is applied to the coil, one end of the coil is at a different voltage than the other end. This difference in voltage from one end of the coil to the other can be several kilovolts in magnitude and can create a large electric field that

induces currents in the sample and thereby heats it.<sup>49</sup> While solenoids are very efficient in producing high  $B_1$  fields, they also generate considerable electric fields that interact with conductive biological samples. This interaction reduces the efficiency of the probe for NMR purposes at the same time as it heats, and possibly damages, the sample. Minimizing the conductivity of the sample will reduce this heating, but the salinity of the sample can be crucial to the conformation of the proteins and so reducing conductivity may not be possible. Fortunately, changing the coil design can alleviate this type of heating. In the case of a solenoid, the voltage and the resultant heating can be reduced by decreasing the number of turns. However, a reduction in the number of turns leads to a less efficient low-frequency observe channel and, therefore, is an undesirable alternative for low sensitivity experiments requiring  $^{13}\text{C}$  or  $^{15}\text{N}$  detection.

Several alternatives to the use of a multiturn solenoid have been proposed to reduce sample heating in biological ssNMR probes. The scroll coil<sup>47,51</sup> is a variation of a multiturn solenoid that not only has a lower inductance, reducing the voltage required to drive current through the coil, but is largely self-screening with respect to the electric field. It also has the significant advantage that it can be tuned and matched through a network very similar to those already in use by probe manufacturers. Unfortunately, its reduced inductance makes it somewhat less sensitive on the lower frequency channels than a traditional solenoid, although for most biological samples the decrease in probe efficiency is outweighed by the reduction in sample loss. More recently, the so-called Z-coil configuration has been proposed that employs a 1/2 turn central portion and pancake coils at each end.<sup>52</sup> The Z-coil appears to reduce heating, but also has lower intrinsic efficiency than simple wire solenoids. However, although both of these approaches keep the electric fields associated with coil self-resonance away from the sample, neither of them particularly mitigates the self-resonance itself. Therefore, the sample size is still limited by the need to keep the electrical length of sample coil to less than one quarter wavelength of the  $^1\text{H}$  resonance.

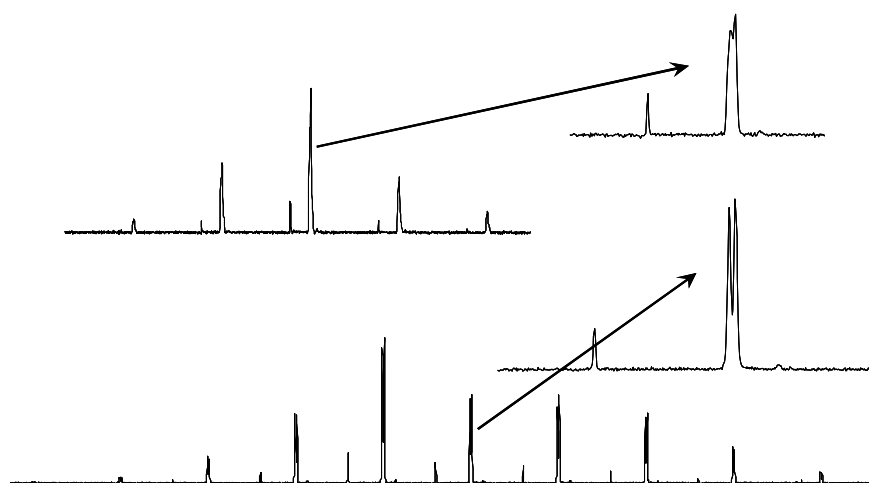


**Figure 1.** 5 kHz  $^{13}\text{C}$  CPMAS spectrum of the carbonyl region for  $^{13}\text{C}'$ -enriched  $^*\text{G}^*\text{GV}$  at 9.4 (top) and 21.1 T (bottom). Inset is an expansion of the isotropic chemical shifts. Increased linewidths for the amide carbonyls at 9.4 T are due to quadrupolar broadening from the  $^{14}\text{N}$  in the amide bonds. Linewidths with and without adjacent  $^{14}\text{N}$  are 80 and 40 Hz at 9.4 T and 65 and 40 Hz at 21 T.

An alternative to the use of a single coil is to use a separate and more appropriate coil for the  $^1\text{H}$  channel in a crossed-coil configuration that reduces electrical interactions between the channels. Probes of this type utilizing a foil saddle coil for the  $^1\text{H}$  channel that is located within an outer, low-frequency solenoid have been produced and successfully used for many years by Doty Scientific, and have been recently described.<sup>48</sup> We have proposed a complementary approach, the 'Low-E coil', which places the low-frequency solenoid within an outer loop-gap resonator (LGR) for the  $^1\text{H}$  channel.<sup>49</sup> Cross-coil probes do have the drawback that the filling factor of either the lower or higher frequency channel must be reduced, although this has not been a significant limitation in practice. They also may not be compatible with matching and tuning networks developed for single-coil probes, and so require additional effort for probe manufacturers. However, while single-coil technologies are limited by self-resonance effects, cross-coil probes allow for the use of high frequency coil designs developed for other applications, such as EPR, which allow for larger sample volumes.

The Low-E probe is based on a combination of a solenoid and an LGR. The LGR<sup>53–56</sup> is a low-inductance alternative to the solenoid. EPR has benefited extensively from the use of LGRs since they exhibit good characteristics at high frequency. However, at lower frequencies their lower inductance leads to a reduction in sensitivity. This problem has been overcome by implementing a crossed-coil design in which an LGR tuned to the proton frequency is used in combination with a solenoid coil tuned to lower frequencies. We have developed and tested this approach for X- $^1\text{H}$  flat coil probes designed for large aligned membrane protein samples at 400, 500, 600, 700, and 900 MHz. A significant advantage of using the LGR for the proton channel is the drop in the electric fields generated in the sample. These resonators reduce the amount of r.f. power dissipated in lossy media by 10–15 $\times$  and ensure sample stability during long demanding experiments.<sup>49</sup> The low-E r.f. coil assembly consists of an LGR and solenoid with a coil volume of  $7.5 \times 5.5 \times 11 \text{ mm}^3$  or  $470 \mu\text{l}$  that produce  $B_1$  fields in orthogonal directions (Fig. 2). The outer  $^1\text{H}$  resonator is slit strategically to cancel low-frequency eddy currents which would otherwise be induced by the inner coil. The LGR produces high, homogeneous  $B_1$

fields at relatively low voltages resulting in an inherently low-E field. The Faraday screening effect of the solenoid further reduces the E-field present in the sample. The r.f. homogeneity produced in the LGR is considerably higher than what can be achieved in a solenoid: a direct benefit for many ssNMR experiments. Each coil is tuned to a single resonance, so the channels are considerably more efficient since there is no need to introduce r.f. traps. Even though the LGR has a significantly lower filling factor, its decoupling efficiency is comparable to that of a single, double-tuned, solenoid, as the 600 MHz probe produces a  $^1\text{H}$   $B_1$  of 100 kHz with a power of 350 W. Furthermore, for a lossy biological sample, the field drops only by 7% instead of 50% as in a comparable solenoid. The use of more turns in the low-frequency solenoid than would have been possible if it were tuned also for  $^1\text{H}$  increases its efficiency and sensitivity; for example, the 600 MHz probe produces a  $^{15}\text{N}$   $B_1$  of 71 kHz for a power input of 700 W, a 37% increase over the double-tuned solenoid.

The r.f. technology developed for oriented sample probes is directly applicable to MAS probes. The only requirement is integrating the sample coils with a MAS stator. Thus, probes optimized for examining dilute proteins in heterogeneous systems via MAS techniques are also possible. We recently constructed a 750 MHz  $^1\text{H}$ - $^{13}\text{C}$  probe for the study of dilute protein samples up to  $80 \mu\text{l}$  in volume (Fig. 3); initial results indicate that this design significantly improves r.f. capabilities at these frequencies without sacrificing lineshape.

Selecting the optimal sample size is one of the primary decisions that must be made in the design of ssNMR probes. The early development of high-field biological ssNMR probes focused on smaller diameter coils that provided good sensitivity for mass-limited samples, strong, homogeneous r.f. fields, and fast sample rotation. Published data for these 2 and 3.2 mm probes (with active volumes of approximately 6 and  $25 \mu\text{l}$ , respectively) have demonstrated that the expected gains in sensitivity and resolution on going to high magnetic fields can be achieved.<sup>47,57</sup> However, with such small rotors, the rotor wall thickness and the gap between the rotor and the coil take a large fraction of the active volume in the coil. Recent work has demonstrated that a detection coil can be placed inside the rotor and inductively coupled

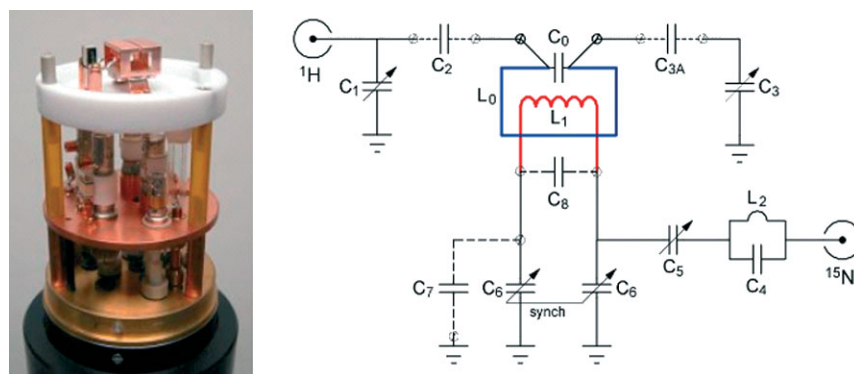


**Figure 2.** Left: 900 MHz  $^1\text{H}$ - $^{15}\text{N}$  probe with  $7.5 \times 5.5 \times 11 \text{ mm}$  coil aperture utilizing a crossed-coil design. The  $^1\text{H}$  coil is a loop gap resonator surrounding the solenoid tuned to the  $^{15}\text{N}$  frequency. Right: The low-E coil assembly consists of a multiturn low-frequency observe solenoid  $L_1$  (red) inside a low-inductance  $^1\text{H}$  loop-gap resonator  $L_0$ - $C_0$  (blue). Dashed lines represent detachable capacitors allowing retuning to other observed nuclei.

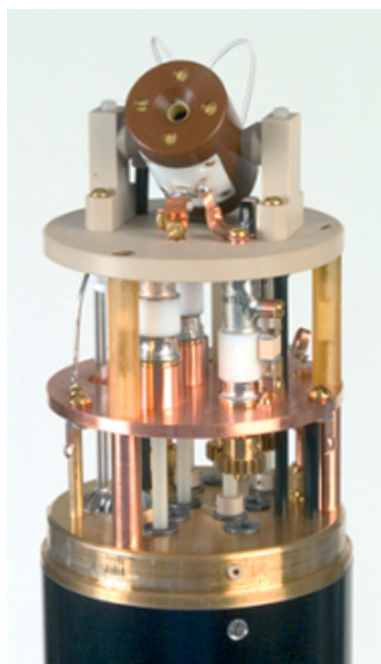


**Figure 3.** 750 MHz  $^1\text{H}$ - $^{13}\text{C}$  MAS probe utilizing a crossed-coil design and circuit similar to the coil and schematic shown in Fig. 2. The coils are seated in a stator designed for 4 mm rotors and supplied by David Lewis of Revolution NMR, LLC, Ft. Collins, CO.

to the external r.f. circuit,<sup>58</sup> but practical application of this technology for biological samples is still under development. Fortunately, crossed-coil approaches now allow for larger sample volumes without the fundamental wavelength limitations of solenoids or scroll coils.

Most membrane proteins of interest, when maintained in a biologically appropriate environment, are quite dilute. For membrane protein samples, in the case of tractable proteins, a lipid : protein ratio of 20 or 30 : 1 can be sufficient; quite often, however, proteins can aggregate even at these concentrations and higher levels of lipids must be used. In order for most proteins to maintain their native structures, samples must be fully hydrated with an appropriate buffer. For amyloidogenic proteins, samples must often be prepared from very dilute solutions if one wishes to examine the process of plaque formation rather than the final stage aggregate. Thus, for many biological problems that stand to gain the greatest insight from ssNMR, the proteins of interest often make up less than 10% of the sample weight. For a small protein (10 kDa), this would mean that a sample containing 100 nmoles (1 mg) of protein would require a sample volume of 10  $\mu\text{l}$  or more under the most ideal conditions. However, 100 nmoles, while sufficient for basic chemical shift and relaxation measurements, is inadequate for most multidimensional and/or multiple quantum NMR experiments. Long signal averaging times also prevent the study of chemically labile systems since sample degradation over the course of the experiment would be significant. With modern molecular biology, it is now possible to generate significantly larger quantities of protein (>1  $\mu\text{mole}$ ) in a single liter of culture. Therefore, for less ideally

behaved protein samples, using a larger sample size enables significantly more ssNMR applications and experiments.

When determining optimal sample size for mass-limited protein samples vs. concentration-limited samples, sensitivity, accessible  $B_1$  fields, and sample spinning requirements must be compared. Figure 4 shows the relative sensitivity for MAS probes with different rotor diameters. To simplify our analysis, we compared typical MAS rotor diameters and assumed: (i) the solenoidal (detection) coil diameter is 0.6 mm greater than the rotor diameter, (ii) the length of each coil is twice its diameter, (iii) a low-E circuit is utilized on the  $^1\text{H}$  channel to minimize wavelength effects, (iv) the rotor has a wall 0.4 mm thick, (v)  $B_1$  homogeneity remains constant since the length/diameter ration is fixed, and (vi) the sample is constrained to 0.8 times the length of the coil to allow reasonable  $B_1$  homogeneity for multipulse experiments. Relative sensitivity per unit volume is calculated as (smallest coil diameter)/(coil diameter) since sensitivity scales inversely with coil diameter when keeping the aspect ratio the same.<sup>59</sup> Sensitivity for a full rotor is calculated as the sensitivity per unit volume times the volume of the rotor. Thus, sensitivity per unit volume scales as  $\sim(1/x)$  with respect to the rotor diameter while full rotor sensitivity scales as  $x^2$ .

From this plot, it is apparent that mass-limited samples are best studied with smaller rotors, but that a significant enhancement in sensitivity is possible for concentration-limited samples by using a larger rotor. The use of low-E probe designs is crucial, as it allows sufficient  $B_1$  to be maintained even over the larger samples. Consequently, we have chosen to focus on the development of ssNMR probes with active sample volumes on the order of 100  $\mu\text{l}$ . Our results with large volume probes tested at 400–900 MHz demonstrate that, although there are significant engineering challenges, the use of larger coils is a feasible way to increase NMR sensitivity for dilute protein systems.<sup>45,49</sup> One drawback of larger volume coils is that the relative power required to generate a  $B_1$  field is the inverse of sensitivity per unit volume squared.<sup>59</sup> Thus, while a full 4 mm rotor will provide more than 7 times the signal of a 2 mm rotor, achieving an equivalent  $B_1$  field will require 4–5 times as

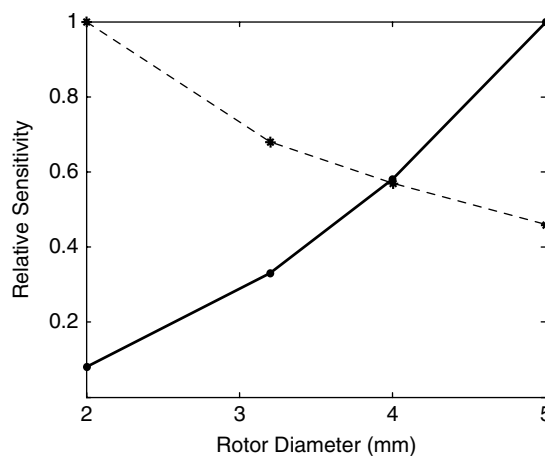


**Figure 4.** Comparison of probe sensitivity for various sample (rotor) sizes. Shown are relative sensitivity per unit volume (---) and relative sensitivity for a full rotor (—).

much power. However, with the low-E design,  $^1\text{H}$  fields of  $>100$  kHz can be attained in a 4 mm rotor within the 300 W available on many spectrometers. A final consideration is that maximum spinning speeds also scale approximately with the inverse of the rotor diameter.

### CHARACTERIZING A BIOLOGICAL SSNMR PROBE

Given the many variables discussed above affecting the performance of ssNMR experiments, serious consideration of how an ssNMR probe should be evaluated is warranted. Typical specifications available from vendors include sample volume, MAS rates, magic angle stability, linewidths on ideal compounds such as a liquid or adamantane, maximum  $B_1$  fields achievable and power input required, maximum pulselength and duty cycle, S/N on a model compound such as glycine, and temperature range. What is also needed in evaluating a probe is a measure of 810/90 for each r.f. channel as a function of sample length and experimental determination of r.f. heating using representative samples and pulse experiments. Once these specifications are known, many of the experimental parameters for particular pulse sequences can be optimized either at the spectrometer or *in silico*.

Unfortunately, with the generation of high  $B_1$  fields comes the correlate generation of high electric fields, which leads to sample heating. Radiofrequency heating of biological macromolecules threatens sample stability,<sup>46,47,60</sup> distorts NMR lineshapes, decreases S/N,<sup>61</sup> and requires longer recycle delays and lower duty cycles, and ultimately can destroy the sample, rendering any measurement irrelevant. Using low-inductance coils such as LGRs or scroll coils is the best method for minimizing this type of heating since they minimize the magnitude of voltage built up on the coil in generating a given  $B_1$  field.

Efficient sample cooling is also important, and accurate temperature measurement is crucial to evaluating probe designs. In implementing ssNMR experiments at high frequencies, every precaution to reduce sample heating must be taken. Thus, some compromises in choice of coil size, r.f. field strength, and experimental duty cycle must be made. When r.f. heating is minimized, not only are protein samples more stable for a selected set of experimental conditions, but the possibility arises that r.f. duty cycles may be increased. In typical ssNMR experiments using multiply resonant solenoids, the duty cycle is kept well below 2% because of r.f. heating concern rather than the inherent  $T_1$  of the system. However, with the reductions in sample heating seen with scroll and low-E probes, it is now possible to significantly increase sample throughput by lowering the delay time between signal acquisitions. A final consideration in exploring membrane proteins is the role of lipid phase transitions and biomolecular dynamics in function; both of these phenomena are highly temperature dependent, so any sample heating due to r.f. irradiation can alter measurements, making them inconsistent or even irrelevant.

If the heat capacity of the sample is known, it is possible to extrapolate its rise in temperature from basic r.f. and

NMR measurements. One can measure the power supplied to produce an identical flip angle in a lossless reference sample relative to the biological sample of interest and assume the difference was converted to thermal energy in the sample. This method is particularly useful when NMR thermometry methods are not well established, such as in mechanically aligned bilayers. Figure 5 shows the difference in decoupler heating between solenoids and low-E probes for such rectangular bilayer samples at a range of magnetic fields and corresponding  $^1\text{H}$  frequency. The low-E probes reduce heating by a factor of about 15 over the entire range. It is apparent that even with low-E probes, an increase in field strength leads to greater heating.

A more direct means to measure the r.f. heating for various sample conditions is to dope samples with thulium 1,4,7,10-tetraazacyclododecane-1,4,7,10-tetrakis(methylene phosphonate) (TmDOTP<sup>5-</sup>) and monitor the chemical shift of the  $\text{H}_6$  peak which is at  $\sim -150$  ppm at ambient temperatures and whose shift is quite sensitive to temperature changes.<sup>47,62</sup> TmDOTP is readily soluble in buffers commonly used to make ssNMR samples, and MAS rotors can be made vapor impermeable through judicious use of PTFE tape or endcaps with O-rings. By spinning at speeds of  $\sim 2$  kHz, one can minimize heating due to spinning while averaging magnetic susceptibility artifacts and mimicking common experimental conditions for air flow. The heating due to r.f. pulses can then be determined by applying a rectangular pulse at the length and power of a normal experiment (typically 40 ms at the highest safe  $^1\text{H}$  power) at the frequency of water ( $\sim 4.7$  ppm) and then observing the  $\text{H}_6$  proton with a simple pulse-acquire sequence after a delay of 15 ms to allow relaxation. By taking the ratio of the measured temperature rise  $\Delta T$  to the time average of  $B_1^2$  over the entire experiment, it is possible to compare

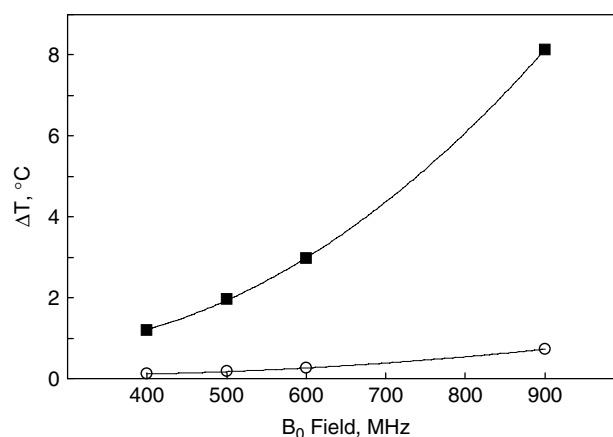


**Figure 5.** Comparison of temperature rise inside a static, mechanically oriented M2-TMD sample following a single 50 kHz, 10 ms long  $^1\text{H}$  decoupling pulse, using solenoid and low-E flat-coil probe designs at various spectrometer fields  $B_0$ . Coils with  $7.5 \times 5.5 \times 11$  mm aperture were used in all cases. Sample: 10 mg M2-TMD and 80 mg DMPC, fully hydrated, in 50 mM acetic acid, pH 4.5. The temperature rise is extrapolated from measurements of the absorbed r.f. power using an average sample heat capacity of  $3.5 \text{ J/g}^\circ\text{C}$ .<sup>46</sup> Shown are results for samples in a solenoid (■) and low-E probe (○).

the sample heating characteristics of probes having different efficiencies. Figure 6 illustrates this technique as used to measure the heating by 4 mm solenoid and low-E MAS probes at 700 MHz using samples of 243 mM saline. The solenoid probe is a commercial TL2 MAS probe by Bruker Biospin (Billerica, MA). The other probe had a low-E coil incorporated inside an identical MAS stator. The graph confirms that sample heating is reduced to an acceptable level in low-E probes even for large samples at high field. It also illustrates that the longer (50  $\mu$ l) samples are more prone to heating in either solenoid or low-E probe than short (10  $\mu$ l) samples. Another less sensitive method of measuring the temperature in biological samples is to monitor the proton chemical shift of water.<sup>63</sup>

A final consideration for temperature regulation in MAS ssNMR is frictional heating caused by sample rotation. A common method for measuring these effects is to monitor the <sup>207</sup>Pb resonance in lead nitrate as a function of spinning speed since it is temperature sensitive.<sup>64,65</sup> In most commercial probes, frictional heating is observable at only a few kHz,<sup>2,3</sup>

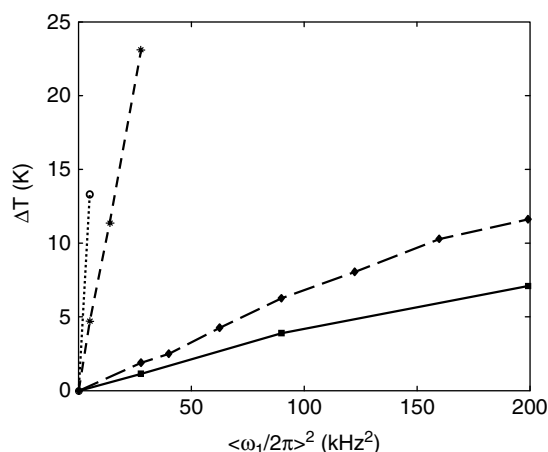


**Figure 6.** Measurements of r.f.-induced sample heating in 4 mm MAS probes for a sample of 243 mM saline. Shown are shorter 10  $\mu$ l samples in a solenoid (\*- - -) and low-E probe (■—) as well as longer 50  $\mu$ l samples in a solenoid (○····) and low-E probe (◆- - -).

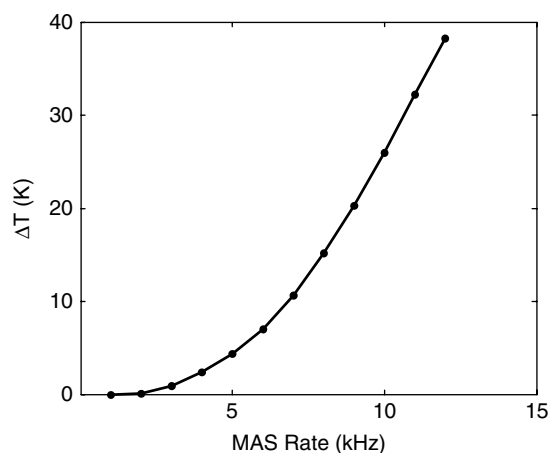


**Figure 7.** Measurements of sample heating due to friction for a sample of lead nitrate in a 4 mm rotor.

and quickly climbs to 20–30 °C at higher spinning speeds (Fig. 7). This heating is not necessarily uniform across the sample. Adjusting the bearing and drive air can significantly affect how much heating occurs and should be optimized to minimize frictional heating for a particular probe at the spinning speeds it will be operated.

## NUMERICAL SIMULATIONS FOR EVALUATING PULSE SEQUENCES AT HIGH FIELD

While through years of experience scientists specializing in ssNMR are able to gain a feel for what the limits of various experiments are with regard to magnetic field, probe capabilities, sample properties, and the desired information, biologists and biophysicists interested in applying ssNMR to their particular research areas are often at a loss as to which experiments to pursue and how to implement them. Numerical simulations, using programs such as SPINEVOLUTION<sup>66</sup> and SIMPSON,<sup>67,68</sup> provide a means of determining which type of experiment and parameters for that experiment will be most useful for a particular research problem. Simulations are especially critical at high fields, as access to high field instrumentation is in high demand and typical run times are on the order of a few hours to a few days which prevent exhaustive calibration of the instrument for a particular set of conditions and experiments. These simulations not only can predict outcomes for ideal r.f. pulses and spin rates, but can also be configured to allow the user to input experimental variables such as the attainable MAS rate (either based on spinning stability or attainable r.f. fields), measured 810/90 for a particular channel, any variations in the r.f. profile between channels, and any incorrectly set parameters such as a frequency offset or CP matching condition allowing exploration of the parameter space encompassed by MAS and the r.f. phase, length, and attainable amplitudes of the different input frequencies. In this way, experiments that prove to yield poor results can be tried without taking up valuable spectrometer time.

With the implementation of higher  $B_0$  fields, chemical shift ranges and dipolar couplings are of the same order of magnitude, as are the r.f. fields and MAS rates manipulating them. Under these conditions, simulations are invaluable learning tools for even simple experiments, such as CP. Figure 8 demonstrates the importance of shaped pulses to compensate for r.f. inhomogeneity and frequency offsets.<sup>69</sup> Shown are the calculated <sup>1</sup>H–<sup>13</sup>C CP efficiencies for either a square or a ramped 3 ms pulse as a function of <sup>1</sup>H r.f. field with the <sup>13</sup>C r.f. field held constant at 50 kHz. These calculations are for a static sample at 750 MHz with a dipole coupling of 2500 Hz. In the initial calculation, neither r.f. channel has inhomogeneity and the spins have isotropic chemical shifts on resonance. In the second calculation, both r.f. channels have inhomogeneity, 75% for <sup>13</sup>C and 95% for <sup>1</sup>H, modeled as in Ref. 44. In the third calculation, the conditions mimic those for a peptide exhibiting limited dynamics in a fluid lipid bilayer: both r.f. channels have inhomogeneity and the <sup>13</sup>C nucleus has a CSA typical of a carbonyl carbon ( $\delta_{\text{aniso}} = -75$  ppm,  $\eta = 0.8$ ). We can see that the ramped pulses produce much higher CP efficiency than square pulses under realistic experimental conditions, and also that the

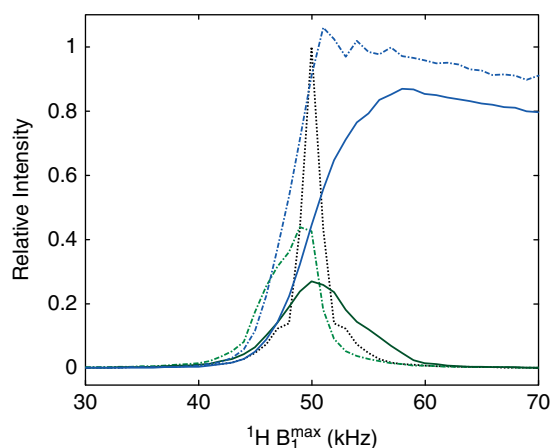


**Figure 8.** CP efficiency for a static sample using ramped and square  $^1\text{H}$  CP r.f. fields with the  $^{13}\text{C}$  field held at 50 kHz and the  $^1\text{H}$  field in the center of the coil as indicated. The black dotted line shows the ideal two-spin behavior with a square CP r.f. pulse. Blue and green plots represent behavior for ramped and square r.f. fields, respectively, in the case of inhomogeneous r.f. without isotropic/anisotropic chemical shift (---) and with the  $^{13}\text{C}$  spin having a CSA typical for a carbonyl carbon (—).

maximum  $B_1$  will need to be about 20% higher than a simple estimate which neglects chemical shift effects. These simulations demonstrate the well-established importance of ramped CP measurements and are instructional to those entering the ssNMR field. Figure 9 shows simulated CPMAS profiles at two spinning speeds using the same conditions as in the final conditions of Fig. 8. At higher spinning speeds (20 kHz), the MAS is sufficiently larger than the dipolar coupling (2500 Hz) and of the same order of magnitude as the r.f., which leads to the dramatic drop in CP efficiency between 60 and 70 kHz  $^1\text{H}$  r.f.

A variety of MAS ssNMR methods have been developed to extract information about local atomic structure in noncrystalline, macroscopically disordered proteins. These

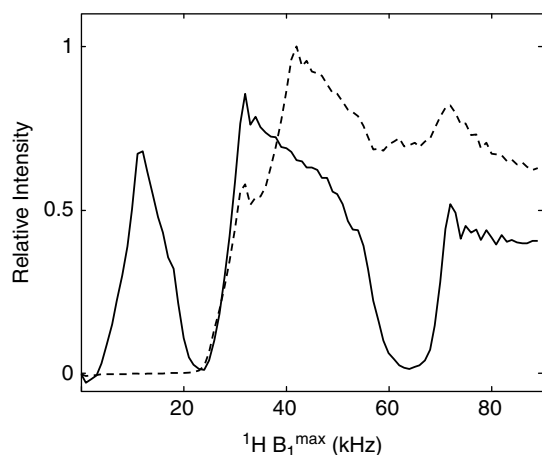


**Figure 9.** Calculated CPMAS intensity at 10 (---) and 20 (—) kHz MAS for a carbonyl carbon at 21.1 T as a function of  $^1\text{H}$  r.f. field in the center of the coil with the  $^{13}\text{C}$  field held at 50 kHz.

methods typically rely on the spin characteristics of rare spin 1/2 nuclei, such as  $^{13}\text{C}$  and  $^{15}\text{N}$ , either in concert with each other or with their directly bonded protons, invariably requiring the incorporation of isotopically enriched amino acids. Extracting backbone secondary structure information can be accomplished by measuring internuclear spin interactions. NMR experiments that focus on internuclear distances or the relative orientations of the dipolar interactions<sup>70–74</sup> and/or relative CSAs<sup>14,75–83</sup> of particular spin networks have been developed and demonstrated to measure backbone secondary structure in peptides and proteins. In applying these experiments at high field, care should be taken to evaluate how these experiments are affected by various parameters, such as relaxation, chemical shift anisotropy, relative spin orientations, and r.f. inhomogeneity. Additionally, for systems in which no prior structural information is available or which have a mixture of conformations, consideration of the labeling schemes and pulse sequences applicable to a wide array of secondary structures is required. Recently we assessed the experimental accuracy and relevance of using  $^{13}\text{C}'(i) \rightarrow ^{13}\text{C}'(i+1)$  interactions to determine backbone torsion angles.<sup>84</sup> This particular pair of spins was chosen owing to their ease of isotopic enrichment, consistent relaxation and CSA characteristics, the sufficiently large size of their interactions, and the lack of redundancy in their relative CSA orientations over the allowed  $\phi, \psi$  torsion angle space.<sup>6,30,75,77,79,80</sup> The DQDRAWS experiment (chosen to select  $^{13}\text{C}'(i) \rightarrow ^{13}\text{C}'(i+1)$  interactions) offers a robust technique (even at high fields and with currently achievable r.f. fields and spinning speeds) for examining these interactions without detrimental effects to biological NMR samples.<sup>85</sup> These being homonuclear interactions, the two-spin coherences can be DQ-filtered, an advantage which obviates corrections for single-quantum interactions from naturally abundant  $^{13}\text{C}$  nuclei with overlapping resonances (Fig. 10).<sup>6,32,86</sup>

For recoupling sequences that require a train of pulses to

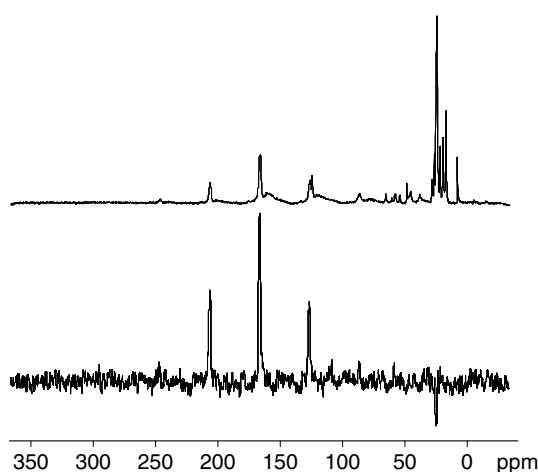


**Figure 10.** CPMAS (top) and DRAWS DQ-filtered (bottom) spectra of a peptide interacting with a complex lipid mixture. The peptide is  $^{13}\text{C}$ -enriched at two adjacent  $\text{C}'$  positions in the peptide backbone to allow for DQ filtering. For two  $^{13}\text{C}'$  spins with a dipolar coupling of 250 Hz, a DQ filtering efficiency of  $\sim 25\%$  can be achieved at 500 MHz.

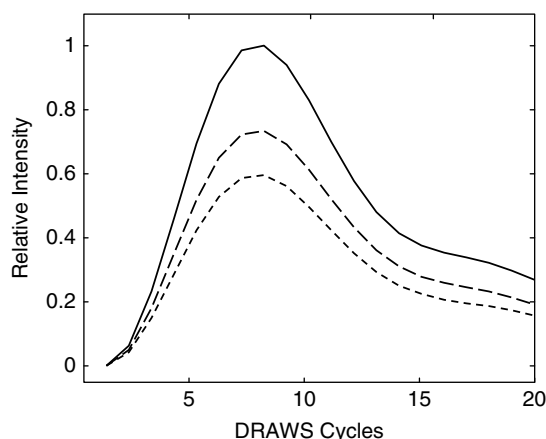


**Figure 11.** DRAWS pulse sequence performance as a function of  $^{13}\text{C}$  r.f. homogeneity at 750 MHz. Shown is the relative intensity of DQ-filtered signal as a function of mixing time. Shown are calculated curves for probes with relative homogeneities (810/90) of 95% (—) 75% (- - -) and 50% (- . - . -).

manipulate the CSAs, the dependence on strong, homogeneous r.f. fields is even more acute. Figure 11 shows the expected results for the buildup of double-quantum coherence between two  $^{13}\text{C}$  carbonyl carbons with a dipolar coupling of 250 Hz using the DRAWS sequence at a spinning speed of 5 kHz at 750 MHz. As is evident in the figure, improving the 810/90 on the carbon channel from 50 to 95% can increase the S/N by a factor of  $\sim 1.7$ . It should be noted that this pulse sequence is more robust than other recoupling sequences with respect to CSAs<sup>85</sup>; thus recoupling sequences such as SPC5 and C7 would benefit further from improvements in the r.f. characteristics of MAS probes. Figure 12 shows a simulation of the maximum DQ signal attainable as a function of r.f. homogeneity and magnetic field.

As NMR spectrometers have converted from analog to digital r.f. technology, it has become possible to develop more sophisticated pulse sequences to overcome some of the limitations imposed by available r.f. technology. The current spectrometers allow sequences of arbitrary phases

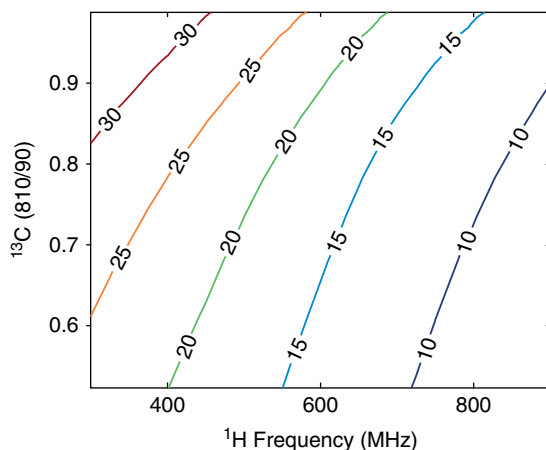


**Figure 12.** Maximum percentage of DQ-filtered signal (relative to CPMAS) from a DRAWS pulse sequence as a function of r.f. homogeneity and magnetic field strength.

and powers with relatively high slew rates. This opens the opportunity for more complicated sequences designed using computer optimization to explore larger parameter spaces in pulse sequence development. Optimization via numerically based simulations has been applied to homonuclear decoupling,<sup>87</sup> heteronuclear decoupling<sup>88</sup> and dipolar recoupling,<sup>89</sup> double quantum excitation,<sup>90</sup> and quadrupolar excitation.<sup>89</sup> Additionally, in some instances optimizing via a feedback loop on a spectrometer rather than a simulator has proven successful.<sup>88</sup>

While Fig. 12 shows that the DRAWS sequence, like many other sequences, is sensitive to both field strength increases and probe homogeneity, numerical optimizations suggest that it is possible to create a pulse sequence that is less sensitive to probe homogeneity and has a higher efficiency as the field strength increases than the DRAWS sequence. Work continues towards improving more complex pulse sequences and complex spin systems via numerical optimization.

### Acknowledgements

We thank Prof. Arthur Edison, Dr Douglas Elliott, and Prof. Manish Mehta for many very helpful discussions in writing this paper. We thank the University of Florida High Performance Computing Center for the use of their cluster of computers for the numerical simulations. Funding was provided by NIH R01 HL076586, the National High Magnetic Field Laboratory in-house research program, and the University of Florida.

### REFERENCES

- Lange A, Giller K, Hornig S, Martin-Eauclaire MF, Pongs O, Becker S, Baldus M. *Nature* 2006; **440**(7086): 959.
- Marassi FM, Ramamoorthy A, Opella SJ. *Proc. Natl. Acad. Sci. U.S.A.* 1997; **94**(16): 8551.
- Mani R, Cady SD, Tang M, Waring AJ, Lehrert RI, Hong M. *Proc. Natl. Acad. Sci. U.S.A.* 2006; **103**(44): 16242.
- van Beek JD, Hess S, Vollrath F, Meier BH. *Proc. Natl. Acad. Sci. U.S.A.* 2002; **99**(16): 10266.
- van Beek JD, Beaulieu L, Schafer H, Demura M, Asakura T, Meier BH. *Nature* 2000; **405**(6790): 1077.
- Long JR, Oyler N, Drobny GP, Stayton PS. *J. Am. Chem. Soc.* 2002; **124**(22): 6297.
- Zech SG, Wand AJ, McDermott AE. *J. Am. Chem. Soc.* 2005; **127**(24): 8618.
- Castellani F, van Rossum B, Diehl A, Schubert M, Rehbein K, Oschkinat H. *Nature* 2002; **420**(6911): 98.
- Castellani F, van Rossum BJ, Diehl A, Rehbein K, Oschkinat H. *Biochemistry* 2003; **42**(39): 11476.
- Igumenova TI, McDermott AE, Zilm KW, Martin RW, Paulson EK, Wand AJ. *J. Am. Chem. Soc.* 2004; **126**(21): 6720.
- Franks WT, Wylie BJ, Stellfox SA, Rienstra CM. *J. Am. Chem. Soc.* 2006; **128**(10): 3154.
- Franks WT, Zhou DH, Wylie BJ, Money BG, Graesser DT, Frericks HL, Sahota G, Rienstra CM. *J. Am. Chem. Soc.* 2005; **127**(35): 12291.
- Wylie BJ, Sperling LJ, Frericks HL, Shah GJ, Franks WT, Rienstra CM. *J. Am. Chem. Soc.* 2007; **129**(17): 5318.
- Rienstra CM, Hohwy M, Mueller LJ, Jaroniec CP, Reif B, Griffin RG. *J. Am. Chem. Soc.* 2002; **124**(40): 11908.
- Martin RW, Zilm KW. *J. Magn. Reson.* 2003; **165**(1): 162.
- Petkova AT, Ishii Y, Balbach JJ, Antzutkin ON, Leapman RD, Delaglio F, Tycko R. *Proc. Natl. Acad. Sci. U.S.A.* 2002; **99**(26): 16742.
- Petkova AT, Leapman RD, Guo ZH, Yau WM, Mattson MP, Tycko R. *Science* 2005; **307**(5707): 262.
- Havlin RH, Tycko R. *Proc. Natl. Acad. Sci. U.S.A.* 2005; **102**(9): 3284.

19. Hoult DI, Richards RE. *J. Magn. Reson.* 1976; **24**(1): 71.
20. Ketchum RR, Roux B, Cross TA. *Structure* 1997; **5**(12): 1655.
21. Opella SJ, Marassi FM, Gesell JJ, Valente AP, Kim Y, Oblatt-Montal M, Montal M. *Nat. Struct. Biol.* 1999; **6**(4): 374.
22. Nevzorov AA, Mesleh MF, Opella SJ. *Magn. Reson. Chem.* 2004; **42**(2): 162.
23. Wu CH, Ramamoorthy A, Opella SJ. *J. Magn. Reson., Ser. A* 1994; **109**(2): 270.
24. Denny JK, Wang JF, Cross TA, Quine JR. *J. Magn. Reson.* 2001; **152**(2): 217.
25. Opella SJ, Nevzorov A, Mesleh MF, Marassi FM. *Biochem. Cell Biol.* 2002; **80**(5): 597.
26. Palczewski K, Kumasaka T, Hori T, Behnke CA, Motoshima H, Fox BA, Le Trong I, Teller DC, Okada T, Stenkamp RE, Yamamoto M, Miyano M. *Science* 2000; **289**(5480): 739.
27. Xiong JP, Stehle T, Diefenbach B, Zhang RG, Dunker R, Scott DL, Joachimiak A, Goodman SL, Arnaout MA. *Science* 2001; **294**(5541): 339.
28. Johansson J, Curstedt T. *Eur. J. Biochem.* 1997; **244**(3): 675.
29. Antharam VC, Elliott DW, Farver RS, Mills FD, Sternin E, Long JR. Surfactant peptide KL4 differentially modulates lipid dynamics in DPPC:POPG and POPC:POPG bilayers, 2007.
30. Drobny GP, Long JR, Karlsson T, Shaw W, Popham J, Oyler N, Bower P, Stringer J, Gregory D, Mehta M, Stayton PS. *Annu. Rev. Phys. Chem.* 2003; **54**: 531.
31. Long JR, Dindot JL, Zebroski H, Kiihne S, Clark RH, Campbell AA, Stayton PS, Drobny GP. *Proc. Natl. Acad. Sci. U.S.A.* 1998; **95**(21): 12083.
32. Long JR, Shaw WJ, Stayton PS, Drobny GP. *Biochemistry* 2001; **40**(51): 15451.
33. Shaw WJ, Long JR, Campbell AA, Stayton PS, Drobny GP. *J. Am. Chem. Soc.* 2000; **122**(29): 7118.
34. Shaw WJ, Long JR, Dindot JL, Campbell AA, Stayton PS, Drobny GP. *J. Am. Chem. Soc.* 2000; **122**(8): 1709.
35. Stayton PS, Drobny GP, Shaw WJ, Long JR, Gilbert M. *Crit. Rev. Oral Biol. Med.* 2003; **14**(5): 370.
36. Bower PV, Louie EA, Long JR, Stayton PS, Drobny GP. *Langmuir* 2005; **21**(7): 3002.
37. Abragam A. *Principles of Nuclear Magnetism*. Oxford University Press: New York, 1983; 614.
38. Maricq MM, Waugh JS. *J. Chem. Phys.* 1979; **70**(7): 3300.
39. Haeblerlin U. *High Resolution NMR in Solids: Selective Averaging*. Academic Press: New York, 1976.
40. Ishii Y, Ashida J, Terao T. *Chem. Phys. Lett.* 1995; **246**(4–5): 439.
41. Hartmann SR, Hahn EL. *Phys. Rev.* 1962; **128**(5): 2042.
42. Cross VR, Hester RK, Waugh JS. *Rev. Sci. Instrum.* 1976; **47**(12): 1486.
43. Engelke F. *Concepts Magn. Reson.* 2002; **15**(2): 129.
44. Paulson EK, Martin RW, Zilm KW. *J. Magn. Reson.* 2004; **171**(2): 314.
45. Gor'kov PL, Chekmenev EY, Fu RQ, Hu J, Cross TA, Cotten M, Brey WW. *J. Magn. Reson.* 2006; **181**(1): 9.
46. Li CG, Mo YM, Hu J, Chekmenev E, Tian CL, Gao FP, Fu RQ, Gor'kov PL, Brey W, Cross TA. *J. Magn. Reson.* 2006; **180**(1): 51.
47. Stringer JA, Bronnimann CE, Mullen CG, Zhou DH, Stellfox SA, Li Y, Williams EH, Rienstra CM. *J. Magn. Reson.* 2005; **173**(1): 40.
48. Doty FD, Kulkarni J, Turner C, Entzminger G, Bielecki A. *J. Magn. Reson.* 2006; **182**(2): 239.
49. Gor'kov PL, Chekmenev EY, Li CG, Cotten M, Buffy JJ, Traaseth NJ, Veglia G, Brey WW. *J. Magn. Reson.* 2007; **185**(1): 77.
50. Gadian DG, Robinson FNH. *J. Magn. Reson.* 1979; **34**(2): 449.
51. Grant SC, Murphy LA, Magin RL, Friedman G. *Ieee Trans. Magn.* 2001; **37**(4): 2989.
52. Dillmann B, Elbayed K, Zeiger H, Weingertner MC, Piotta M, Engelke F. *J. Magn. Reson.* 2007; **187**: 10.
53. Froncisz W, Hyde JS. *J. Magn. Reson.* 1982; **47**(3): 515.
54. Mehdizadeh M, Ishii TK, Hyde JS, Froncisz W. *Ieee Trans. Microw. Theory Tech.* 1983; **31**(12): 1059.
55. Larsen FH, Daugaard P, Jakobsen HJ, Nielsen NC. *J. Magn. Reson., Ser. A* 1995; **115**(2): 283.
56. Alecci M, Nicholson I, Lurie DJ. *J. Magn. Reson., Ser. B* 1996; **110**(1): 82.
57. Martin RW, Paulson EK, Zilm KW. *Rev. Sci. Instrum.* 2003; **74**(6): 3045.
58. Sakellariou D, Le Goff G, Jacquinet JF. *Nature* 2007; **447**(7145): 694.
59. Webb AG. *Prog. Nucl. Magn. Reson. Spectrosc.* 1997; **31**: 1.
60. Wang AC, BAX A. *J. Biomol. NMR* 1993; **3**(6): 715.
61. Kugel H. *J. Magn. Reson.* 1991; **91**(1): 179.
62. Zuo CS, Metz KR, Sun Y, Sherry AD. *J. Magn. Reson.* 1998; **133**(1): 53.
63. Dvinskikh SV, Yamamoto K, Durr UH, Ramamoorthy A. *J. Magn. Reson.* 2007; **184**(2): 228.
64. Bielecki A, Burum DP. *J. Magn. Reson., Ser. A* 1995; **116**(2): 215.
65. Dybowski C, Neue G. *Prog. Nucl. Magn. Reson. Spectrosc.* 2002; **41**(3–4): 153.
66. Veshtort M, Griffin RG. *J. Magn. Reson.* 2006; **178**(2): 248.
67. Bak M, Rasmussen JT, Nielsen NC. *J. Magn. Reson.* 2000; **147**(2): 296.
68. Bak M, Schultz R, Vosegaard T, Nielsen NC. *J. Magn. Reson.* 2002; **154**(1): 28.
69. Metz G, Wu XL, Smith SO. *J. Magn. Reson., Ser. A* 1994; **110**(2): 219.
70. Reif B, Hohwy M, Jaroniec CP, Rienstra CM, Griffin RG. *J. Magn. Reson.* 2000; **145**(1): 132.
71. Hong M, Gross JD, Griffin RG. *J. Phys. Chem. B* 1997; **101**(30): 5869.
72. Ladizhansky V, Veshtort M, Griffin RG. *J. Magn. Reson.* 2002; **154**(2): 317.
73. Costa PR, Gross JD, Hong M, Griffin RG. *Chem. Phys. Lett.* 1997; **280**(1–2): 95.
74. Feng X, Eden M, Brinkmann A, Luthman H, Eriksson L, Graslund A, Antzutkin ON, Levitt MH. *J. Am. Chem. Soc.* 1997; **119**(49): 12006.
75. Tycko R, Weliky DP, Berger AE. *J. Chem. Phys.* 1996; **105**(18): 7915.
76. Gabrys CM, Yang J, Weliky DP. *J. Biomol. NMR* 2003; **26**(1): 49.
77. Weliky DP, Tycko R. *J. Am. Chem. Soc.* 1996; **118**(35): 8487.
78. Gregory DM, Mehta MA, Shiels JC, Drobny GP. *J. Chem. Phys.* 1997; **107**(1): 28.
79. Bower PV, Oyler N, Mehta MA, Long JR, Stayton PS, Drobny GP. *J. Am. Chem. Soc.* 1999; **121**(36): 8373.
80. Blanco FJ, Tycko R. *J. Magn. Reson.* 2001; **149**(1): 131.
81. Hong M, Griffin RG. *Biophys. J.* 1998; **74**(2): A296.
82. Hong M, Gross JD, Hu W, Griffin RG. *J. Magn. Reson.* 1998; **135**(1): 169.
83. Chan JCC, Tycko R. *J. Am. Chem. Soc.* 2003; **125**(39): 11828.
84. Mehta MA, Eddy MT, McNeill SA, Mills FD, Long JR. *J. Am. Chem. Soc.* 2008; In press.
85. Karlsson T, Popham JM, Long JR, Oyler N, Drobny GP. *J. Am. Chem. Soc.* 2003; **125**(24): 7394.
86. Gregory DM, Wolfe GM, Jarvie TP, Shiels JC, Drobny GP. *Mol. Phys.* 1996; **89**(6): 1835.
87. Sakellariou D, Lesage A, Hodgkinson P, Emsley L. *Chem. Phys. Lett.* 2000; **319**(3–4): 253.
88. De Paepe G, Hodgkinson P, Emsley L. *Chem. Phys. Lett.* 2003; **376**(3–4): 259.
89. Kehlet C, Vosegaard T, Khaneja N, Glaser SJ, Nielsen NC. *Chem. Phys. Lett.* 2005; **414**(1–3): 204.
90. Tosner Z, Glaser SJ, Khaneja N, Nielsen NC. *J. Chem. Phys.* 2006; **125**: Art. No. 184502.